Experiences With a Two-Terminal-Pair Digital Impedance Bridge

Experiences with a two terminal-pair digital impedance bridge

Luca Callegaro, Vincenzo D'Elia, Marian Kampik, Dan Bee Kim, Massimo Ortolano, and Faranak Pourdanesh

Abstract

This paper describes the realization of a two terminal-pair digital impedance bridge and the test measurements performed with it. The bridge, with a very simple architecture, is based on a commercial two-channel digital signal synthesizer and a synchronous detector. The bridge can perform comparisons between impedances having arbitrary phase and magnitude ratio. Bridge balance is achieved automatically in less than a minute. R-C comparisons with calibrated standards, at kHz frequency and $100\,\mathrm{k}\Omega$ magnitude level, give ratio errors of the order of 10^{-6}, with potential for further improvements.

Index Terms

Metrology, impedance, admittance, measurement standards, precision measurements, bridge circuits.

I. Introduction

COAXIAL transformer bridges [1], [2] achieve ultimate accuracy in the measurement of impedance ratios in the audio frequency range, and are widely employed in primary metrology laboratories for the realization of electrical resistance and capacitance units and scales. The main drawbacks of such bridges are the number of available measuring points, typically restricted to decadic purely real or imaginary ratios, and the fact that they typically require manual operation. On the other hand, electronic commercial impedance meters (LCR bridges) allow the quick measurement of impedances having arbitrary magnitude and phase angle, but with relative accuracies limited to the 10^{-4} range, at best.

Digital bridges [3, Ch. 5] employ digital signal sources as ratio standards to allow the comparison of impedances with arbitrary complex ratios, and can be easily automated. These kind of bridges can therefore provide a way to

Luca Callegaro, Vincenzo D'Elia are with the Electromagnetism Division of the Istituto Nazionale di Ricerca Metrologica (INRIM), strada delle Cacce 91, 10135 Torino, Italy. E-mail: l.callegaro@inrim.it.

Marian Kampik is with the Silesian University of Technology, Poland.

Dan Bee Kim is with KRISS - Korea Research Institute of Standards and Science, Daejeon, Korea.

Massimo Ortolano and Faranak Pourdanesh are with the Politecnico di Torino, Torino, Italy, and with INRIM.

Manuscript received January 23, 2015.

calibrate impedance standards having arbitrary magnitude and phase angle, which are suitable to be employed in the verification of LCR bridges.

We have implemented a coaxial voltage ratio bridge to perform comparisons of two terminal-pair impedance standards. This bridge, introduced in [4], is here described in full detail, together with test measurements and an expression of the measurement uncertainty.

[Fig. 1 about here.]

II. Principle of operation

A. Bridge principle

The schematic diagram of the bridge, well known in the literature (see [3, Ch. 5] and references therein; [5], [6]), is given in Fig. 1. The source output channel E_1 drives the impedance Z_A (admittance $Y_\mathrm{A} = 1/Z_\mathrm{A}$); channel E_2, the impedance Z_B (admittance $Y_\mathrm{B} = 1/Z_\mathrm{B}$). Z_A and Z_B are in series and the null detector D senses the common voltage at the low terminals of Z_A and Z_B. The bridge balance condition $V_\mathrm{D} = 0, I_\mathrm{D} = 0$ is achieved by adjusting the amplitude and the phase of one of the two channels. At equilibrium, $E_1 Y_\mathrm{A} + E_2 Y_\mathrm{B} = 0$: this implies that the complex impedance ratio $W = Z_\mathrm{A}/Z_\mathrm{B}$ is given by

$$W = \frac{Z_\mathrm{A}}{Z_\mathrm{B}} = -\frac{E_1}{E_2}\,. \tag{1}$$

The pair E_1, E_2 constitutes the bridge reading.

B. Measurement model

The schematic diagram of Fig. 1 represents an idealized bridge. Fig. 2, instead, shows a circuit model which takes into account the source output impedances and the stray capacitances of the impedance standards in two-terminal pair definition.

[Fig. 2 about here.]

Assuming that the impedances under comparison are defined at the end of the connecting cables, they can be modeled as two-port Π networks [2, Sec. 5.3.6]. Each Π network comprises the high-to-low transadmittance Y_X (where $\mathrm{X} = \mathrm{A}, \mathrm{B}$), the high-to-shield admittance y_HX and the low-to-shield admittance y_LX. Typically, y_HX and y_LX can be regarded as purely capacitive, with an equivalent capacitance of the order of $100\,\mathrm{pF}$.

Each channel $k = 1, 2$ can be modeled with a Thévenin equivalent circuit [7] composed of an ideal voltage source $E_{k\mathrm{X}}$ in series with an output impedance z_k. At equilibrium, when the source k is connected to the impedance Y_X, the channel output voltage $V_{k\mathrm{X}}$ is

$$V_{k\mathrm{X}} = \frac{1}{1 + z_k\left(Y_\mathrm{X} + y_\mathrm{HX}\right)} E_{k\mathrm{X}}. \tag{2}$$

It is well known [8] [9, Sec. 8.7] [2, Sec. 7.4.3] that exchanging the standards under comparison in the bridge arms can correct some of the systematic errors. We call *forward* (F) the configuration where Y_A is connected to

source channel 1 and Y_B to channel 2; *reverse* (R) the configuration where Y_A is connected to channel 2 and Y_B to channel 1. The equilibrium conditions for the two configurations can be written as

$$\begin{aligned} W &= -\frac{V_{1\mathrm{A}}}{V_{2\mathrm{B}}} = -\frac{E_{1\mathrm{A}}}{E_{2\mathrm{B}}}\left(\frac{1+z_2\left(Y_\mathrm{B}+y_\mathrm{HB}\right)}{1+z_1\left(Y_\mathrm{A}+y_\mathrm{HA}\right)}\right) \quad \text{(F)}, \\ W &= -\frac{V_{2\mathrm{A}}}{V_{1\mathrm{B}}} = -\frac{E_{2\mathrm{A}}}{E_{1\mathrm{B}}}\left(\frac{1+z_1\left(Y_\mathrm{B}+y_\mathrm{HB}\right)}{1+z_2\left(Y_\mathrm{A}+y_\mathrm{HA}\right)}\right) \quad \text{(R)}. \end{aligned} \tag{3}$$

Because of source imperfection, the actual ratio E_1/E_2 deviates from the reading $E_1^{(\mathrm{r})}/E_2^{(\mathrm{r})}$. We model this deviation with a complex gain tracking error g, dependent on the channel setting:

$$\frac{E_1^{(\mathrm{r})}}{E_2^{(\mathrm{r})}} = (1+g)\frac{E_1}{E_2}\,. \tag{4}$$

By taking the geometric average of the forward and the reverse bridge readings, the measurement model can be written as

$$W = \left[\frac{1+g_\mathrm{R}}{1+g_\mathrm{F}}\,\frac{E_{1\mathrm{A}}^{(\mathrm{r})}}{E_{2\mathrm{B}}^{(\mathrm{r})}}\,\frac{E_{2\mathrm{A}}^{(\mathrm{r})}}{E_{1\mathrm{B}}^{(\mathrm{r})}} \times \frac{1+z_2\left(Y_\mathrm{B}+y_\mathrm{HB}\right)}{1+z_1\left(Y_\mathrm{A}+y_\mathrm{HA}\right)}\,\frac{1+z_1\left(Y_\mathrm{B}+y_\mathrm{HB}\right)}{1+z_2\left(Y_\mathrm{A}+y_\mathrm{HA}\right)}\right]^{\frac{1}{2}}, \tag{5}$$

where g_F and g_R are respectively the forward and reverse gain tracking errors. Eq. (5) actually yields two values: the choice of the proper branch for the square root should be made according to the nominal value of W.

Under the assumptions that $|g_\mathrm{F}|, |g_\mathrm{R}| \ll 1$ and that all terms $|z(Y+y_\mathrm{H})| \ll 1$, Eq. (5) can be linearized as

$$W = W^{(\mathrm{r})}(1+\epsilon_W)\,, \tag{6}$$

where

$$W^{(\mathrm{r})} = \left[\frac{E_{1\mathrm{A}}^{(\mathrm{r})}}{E_{2\mathrm{B}}^{(\mathrm{r})}}\,\frac{E_{2\mathrm{A}}^{(\mathrm{r})}}{E_{1\mathrm{B}}^{(\mathrm{r})}}\right]^{\frac{1}{2}} \tag{7}$$

is the ratio reading and

$$\epsilon_W = -\frac{1}{2}\Delta g_\mathrm{FR} + \frac{1}{2}\left(z_1+z_2\right)\left[\left(Y_\mathrm{B}+y_\mathrm{HB}\right)-\left(Y_\mathrm{A}+y_\mathrm{HA}\right)\right], \tag{8}$$

with $\Delta g_\mathrm{FR} = g_\mathrm{F} - g_\mathrm{R}$, is a correction term which accounts for the bridge nonidealities.

Eq. (6) shows, as expected, that even a significant but setting-independent gain tracking error g is compensated by averaging the two readings, whereas the error due to the output impedance is in general not compensated, even in 1:1 comparisons, because of the presence of the y_HX terms.

III. Implementation

A coaxial schematic diagram of the bridge is given in Fig. 3; Fig. 4 shows a picture of the assembly.

[Fig. 3 about here.]

[Fig. 4 about here.]

The devices employed in this realization are:

Source (S). Aivon Oy DualDAC (2 channels, 16 bit resolution, up to 5 MS/s maximum sampling rate, 2^{14} maximum sample buffer size; the digital part is optically isolated from the analog one).

Detector (D). Stanford Research mod. 830 lock-in amplifier; an optical output from the source provide the reference signal.

Equalizers (E). Coaxial equalizers on nanocrystalline ferromagnetic cores.

Amplitude and phase of each channel are adjusted by recalculating and uploading new waveform samples. Each sample code is chosen to minimize the quantization error. More refined synthesis strategies can be implemented to improve the resolution [10]. The source implements a double buffer, which allows continuous output even during the upload of a new sample set. The quantities $E_{1\mathrm{X}}^{(\mathrm{r})}$, $E_{2\mathrm{X}}^{(\mathrm{r})}$ which appear in (7) are calculated from the Fourier expansions of the quantized waveforms.

The control program adjusts the source S and reads the detector D via a GPIB interface; it is written in C language under the LabWindows/CVI© environment. At start-up, the user should set the source sampling rate and the number of samples per sine wave period. The user can then set the initial amplitudes (relative to the full-scale defined by the DAC reference voltage) and phases of the two output channels. The bridge equilibrium can be achieved either by manually adjusting the settings of one channel or, more conveniently, by invoking an automatic balancing routine. This routine, described in detail in Ref. [11, Sec. IV], operates iteratively: after reading D, it recalculates the channel settings by means of a root-finding algorithm based on the secant's method. Each iteration has a duration which mainly depends on the detector's time constant, but further delays are introduced when D performs an automatic range adjustment. The duration of a typical iteration is of about 1 s. The balancing routine stops when the voltage magnitude detected by D falls below a predefined threshold. The total adjustment time is typically less than 1 min.

IV. Experimental

A. Some properties of the source employed

In model (6)–(8), the parameters which account for source nonidealities are z_1, z_2 and Δg_{FR}.

The impedances z_1 and z_2 were measured with an LCR meter Agilent mod. 4284A; for frequency f up to about 20 kHz, the output impedance z_k can be modelled with a resistance $r_k = 100(50)\,\mathrm{m\Omega}$ in series with an inductance $l_k = 4(1)\,\mu\mathrm{H}$, $z_k = r_k + \mathrm{j}2\pi f l_k$.

The term Δg_{FR} has undergone a preliminary evaluation [12] for W ratios close to -1. The span of $|\Delta g_{\mathrm{FR}}|$ is less than 2×10^{-6} for $W \approx -1$ within a range of 2×10^{-4}. Δg_{FR} becomes more significant for values of $|W|$ far from unity; however, a full characterization of this parameter has not yet been completed.

Other nonidealities not considered in the model of Sec. II-B were evaluated and found negligible. The relative stability of E_1/E_2 over time of the source employed was tested with the bridge itself, by substituting the impedance standards with an inductive voltage divider (which has a negligible ratio drift). Results are reported in [13]; the Allan deviation of the amplitude ratio at 1 kHz is $10\,\mathrm{nV\,V^{-1}}$ over 30 min; phase difference fluctuations are dominated by

flicker noise beyond $100\,\mathrm{s}$, with an Allan deviation of $40\,\mathrm{nrad}$. The crosstalk between the channels is lower than $-125\,\mathrm{dB}$ up to $16\,\mathrm{kHz}$.

B. Impedance measurements

The bridge was tested with the impedance standards listed in Tab. I, calibrated as two terminal-pair standards (at the end of the connecting cables).

[TABLE 1 about here.]

[TABLE 2 about here.]

Tab. II reports the measurement results. For each comparison, the reported values are:

- The types and the nominal values of the impedances Z_A and Z_B;
- The measurement frequency f chosen to have an angular frequency close to a decadic value;
- The real and the imaginary parts of W as computed from the measurement model (the operators Re and Im denote the real and the imaginary parts, respectively); $|W| \approx 1$ for all measurements;
- A reference ratio $W^\mathrm{ref} = Z_\mathrm{A}^\mathrm{ref}/Z_\mathrm{B}^\mathrm{ref}$ calculated from values $Z_\mathrm{A}^\mathrm{ref}$ and $Z_\mathrm{B}^\mathrm{ref}$ obtained by independent two-terminal pair calibrations traceable to the national standards of capacitance and resistance;
- The real and the imaginary parts of the deviation $\delta = W - W^\mathrm{ref}$ of the bridge measurement from the reference ratio.

Comments:

- In C-C comparisons, $\mathrm{Re}\,W$ is related to the capacitance ratio, while $\mathrm{Im}\,W$ is related to the difference of the phase angles.
- In R-C comparisons, $\mathrm{Im}\,W$ is related to the principal parameter of the impedances (the resistance and the capacitance), whereas $\mathrm{Re}\,W$ is related to the secondary parameter (i.e., the resistor time constant and the capacitor phase angle); the fact that $\mathrm{Re}\,\delta > \mathrm{Im}\,\delta$ can be possibly due to the mediocre knowledge of these secondary parameters, for which INRIM does not have primary national standards.
- For the comparison in row 7 of Tab. II between a $100\,\mathrm{k\Omega}$ resistor and $1\,\mathrm{nF}$ capacitor at the frequency of $1592.36\,\mathrm{Hz}$, a complete uncertainty evaluation has been carried out and it is described in Sec. V.
- The other comparisons listed in Tab. II show that the magnitude of δ is minimum for $W \approx 1 + \mathrm{j}0$ and frequencies in the kHz range or below, while it increases for purely imaginary values of W and for higher frequencies. Even though a full uncertainty evaluation for these comparisons has not been carried out, the behaviour of the deviation is expected because both the uncertainties of W and W^ref strongly depend on W (see also Sec. V), on the values of the impedances and on the measurement frequency.

V. Uncertainty

Since the measurement model (6)–(8) is a complex-valued function of complex-valued input quantities, an expression of the bridge measurement uncertainty has to be carried out in the context of the Supplement 2

of the *Guide to the expression of uncertainty in measurement* [14]. The calculations were performed with the `Metas.UncLib` [15] software package.

An example of uncertainty budget is reported in Tab III for a comparison between a $100\,\mathrm{k}\Omega$ resistor and $1\,\mathrm{nF}$ capacitor at the frequency of $1592.36\,\mathrm{Hz}$, which corresponds to $W \approx 0 + \mathrm{j}1$. The agreement between W and W^{ref} is expressed by the deviation δ and its uncertainty, reported for this case in last row of Tab III: the real and imaginary parts of δ are compatible with zero within an interval of confidence corresponding to a coverage factor of about 2.

Some notes about the evaluation of the uncertainties of the model input quantities:

- The measurements of Tab. II and the uncertainty budget of Tab. III correspond to $|W| \approx 1$, for which we have a characterization of Δg_{FR}. We assigned $\Delta g_{\mathrm{FR}} = 0$ with an uncertainty compatible with the source specifications given in Sec. IV-A.
- Y_{A} and Y_{B} are known from their nominal values, with negligible uncertainty for what concerns the correction term ϵ_W given by (8);
- y_{HA} and y_{HB} include also the connections, and are considered as pure capacitances, $y_{\mathrm{HX}} = \mathrm{j}2\pi f c_{\mathrm{HX}}$, with $c_{\mathrm{HX}} = 200\,\mathrm{pF}$; an uncertainty is included to take into account variations in cable lengths and differences between models;
- The uncertainty of $W^{(\mathrm{r})}$ is the type A uncertainty related to the measurement repeatability.

[TABLE 3 about here.]

The uncertainty expression can be extended to arbitrary W values provided that sufficient information about the input quantities is given. As an example, Fig. 5 shows a color plot of the magnitude $|u(W)|/|W|$ as a function of W, calculated for $Z_{\mathrm{B}} = 100\,\mathrm{k}\Omega$, z_k and y_{HX} as given in Tab. III, and $|W|$ between 0.1 and 10; for convenience the plot is given as a Smith chart, that is, the cartesian coordinates correspond to the conformal mapping $(W-1)/(W+1)$. Since, at the moment, the characterization of Δg_{FR} is not complete, the plot does not take into account this specific contribution. Indeed, different values of Z_{B}, z_k and y_{HX} will lead to a different but analog plot. In particular, the uncertainty is expected to increase toward lower values of $|W|$ because, for fixed Z_{B}, Z_{A} decreases.

[Fig. 5 about here.]

VI. Conclusions

The digital coaxial voltage ratio bridge realized allows to measure two terminal-pair impedances having arbitrary magnitude ratio and phase difference in the audio frequency range.

The development of this bridge is part of the European Metrology Research Programme (EMRP) Project SIB53 AIM QuTE, *Automated impedance metrology extending the quantum toolbox for electricity*. Deliverables of the project include the development of more accurate digital sources which will increase the accuracy of the bridge here described, and interlaboratory comparisons with special standards that will allow the validation of the bridge measurements.

ACKNOWLEDGMENT

The authors are indebted with Jaani Nissilä, MIKES, Finland, for help in the set-up of the bridge.

The activity has been partially financed by Progetto Premiale MIUR[1]-INRIM P4-2011 *Nanotecnologie per la metrologia elettromagnetica* and P6-2012 *Implementation of the new International System (SI) of Units*. The work has been realized within the EMRP Project SIB53 AIM QuTE, *Automated impedance metrology extending the quantum toolbox for electricity*. The EMRP is jointly funded by the EMRP participating countries within EURAMET and the European Union.

REFERENCES

[1] B. P. Kibble and G. H. Rayner, *Coaxial AC bridges*. Bristol, UK: Adam Hilger Ltd., 1984.

[2] S. Awan, B. Kibble, and J. Schurr, *Coaxial Electrical Circuits for Interference-Free Measurements*, ser. IET Electrical Measurement. Institute of Engineering and Technology, 2010, ISBN: 9781849190695.

[3] L. Callegaro, *Electrical impedance: principles, measurement, and applications*, ser. in Sensors. Boca Raton, FL, USA: CRC press: Taylor & Francis, 2013, iSBN: 978-1-43-984910-1.

[4] L. Callegaro, V. D'Elia, and F. Pourdanesh, "Experiences with a two terminal-pair digital impedance bridge," in *Conf. Precision Electromagn. Meas. (CPEM)*, Rio de Janeiro, Brazil, 24–29 Aug 2014.

[5] D. B. Kim, K.-T. Kim, M.-S. Kim, K. M. Yu, W.-S. Kim, and Y. G. Kim, "All-around dual source impedance bridge," in *Conf. Precision Electromagn. Meas. (CPEM)*, Washington DC, USA, 1-6 Jul 2012, pp. 592–593.

[6] J. Lan, Z. Zhang, Z. Li, Q. He, J. Zhao, and Z. Lu, "A digital compensation bridge for R-C comparisons," *Metrologia*, vol. 49, no. 3, p. 266, 2012.

[7] C. A. Desoer and E. S. Kuh, *Basic circuit theory*. Singapore: McGraw-Hill, Inc., 1969.

[8] W. J. Shackelton, "Impedance-measuring bridge," U.S. Patent US1 695 032A, Dec 11, 1928.

[9] B. Hague, *Alternating current bridge methods*, 6th ed. London, UK: Pitman Publishing Ltd, 1971, revised by T. R. Foord and S. T. Mackay.

[10] M. Kampik, "Analysis of the effect of DAC resolution on AC voltage generated by digitally synthesized source," *IEEE Trans. Instrum. Meas.*, vol. 63, pp. 1235–1243, 2014.

[11] L. Callegaro, "On strategies for automatic bridge balancing," *IEEE Trans. Instr. Meas.*, vol. 54, no. 2, pp. 529–532, Apr 2005.

[12] M. Kampik and J. Nissilä, "SIB53 AIM QuTE visit report," MIKES, Tech. Rep., 2014.

[13] J. Nissilä, K. Ojasalo, M. Kampik, J. Kaasalainen, V. Maisi, M. Casserly, F. Overney, A. Christensen, L. Callegaro, V. D'Elia, N. T. M. Tran, F. Pourdanesh, M. Ortolano, D. B. Kim, J. Penttilä, and L. Roschier, "A precise two-channel digitally synthesized AC voltage source for impedance metrology," in *Conf. Precision Electromagn. Meas. (CPEM)*, Rio de Janeiro, Brazil, 24-29 Aug 2014.

[14] "JCGM 102:2011, Evaluation of measurement data — Supplement 2 to the "Guide to the expression of uncertainty in measurement" — Extension to any number of output quantities," 2011. [Online]. Available: http://www.bipm.org

[15] M. Zeier, J. Hoffmann, and M. Wollensack, "*Metas.UncLib*—a measurement uncertainty calculator for advanced problems," *Metrologia*, vol. 49, no. 6, p. 809, 2012.

[16] L. Callegaro, V. D'Elia, and D. Serazio, "10-nF capacitance transfer standard," *IEEE Trans. Instr. Meas.*, vol. 54, no. 5, pp. 1869–1872, 2005.

[1] *Ministero dell'Istruzione, dell'Università e della Ricerca.*

Luca Callegaro (1967) holds a degree in Electronic Engineering (1992) and a Ph.D. in Physics (1996) from Politecnico di Milano, Italy. He joined the Istituto Nazionale di Ricerca Metrologica, INRIM (formerly Istituto Elettrotecnico Nazionale Galileo Ferraris, IEN), Torino, Italy, in 1996. He has been member of the Scientific Council of IEN (1998-2005), adjunct professor of electronic measurements at Politecnico di Torino, Italy. He is responsible of research activity on electrical impedance at INRIM, and of the Italian National standards of electrical capacitance, inductance, ac resistance and ac voltage ratio. He is the Italian contact person of EURAMET TC-EM and member of its Working Group on Strategic Planning. He is the Italian deputy officer for the Commission A of URSI. He is author of about 70 papers on international reviews and of the book *Electrical impedance: principles, measurement and applications* (Taylor & Francis, 2012).

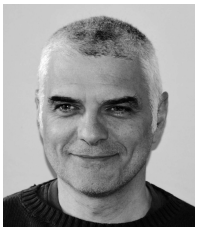

Vincenzo D'Elia was born in Torino, Italy, in 1965. He received the high school degree in electronics in 1988. After working with a telecommunication company, in 1996 he joined the Department of Electrical Metrology, Istituto Elettrotecnico Nazionale Galileo Ferraris (IEN), now Istituto Nazionale di Ricerca Metrologica (INRIM), Torino. He is currently involved in impedance, inductive voltage ratio and low current measurements.

Marian Kampik received the M.Sc., Ph.D., and Habilitate Doctorate degrees in electrical engineering from the Silesian University of Technology, Gliwice, Poland, in 1988, 1996, and 2010, respectively. He has been with the Institute of Measurement Science, Electronics and Control, Faculty of Electrical Engineering, Silesian University of Technology, since 1988, where he became a University Professor in 2010, and the Director of the Institute in 2012. From 1993 to 1995, he was a Visiting Scientist with Physikalisch-Technische Bundesanstalt (PTB), Braunschweig, Germany. His current research interests include AC voltage and current standards, thermal converters, digital signal synthesis, and impedance measurements. Dr. Kampik received the Siemens Prize (team) in 2003, the Research Excellence Grant granted by the European Research Metrology Programme in 2013 and scholarships granted by the German Academic Exchange Service (DAAD) in 1993-95 and 1999.

Dan Bee Kim (1981) received the B.S. in physics from Yonsei University in Seoul, Korea (2004) and the Ph.D. degree in physics from Korea Advanced Institute of Science and Technology in Daejeon, Korea (2010). She joined Korea Research Institute of Standards and Science in 2010, and her research has been focused on the low frequency impedance (electrical capacitance, inductance, ac resistance, and ac voltage ratio).

Massimo Ortolano (1969) received the MSc degree in Electronic Engineering in 1997 and the PhD in metrology in 2001, both from the Politecnico di Torino. Currently, he is a researcher with the Dipartimento di Elettronica e Telecomunicazioni at the Politecnico di Torino, where he is in charge of several courses about electronic measurements. He collaborates with the Istituto Nazionale di Ricerca Metrologica (INRIM) on noise metrology, modelling of quantum Hall effect devices, impedance metrology and electrolytic conductivity measurements. Other reasearch interests are fundamental constants and time and frequency metrology.

Faranak Pourdanesh (1983) was born in Shiraz, Iran, where she graduated (BSc) in Electronic Engineering in 2007, from the Shiraz University. She then moved to Italy where, in 2014, she graduated (MSc) in Electronic Engineering from the Politecnico di Torino, with a thesis on digital bridges for primary impedance metrology. She is currently working towards her PhD in Metrology at the Politecnico di Torino and at the Istituto Nazionale di Ricerca Metrologica (INRIM), having activities in several projects related to the metrology of electrical impedance.

LIST OF FIGURES

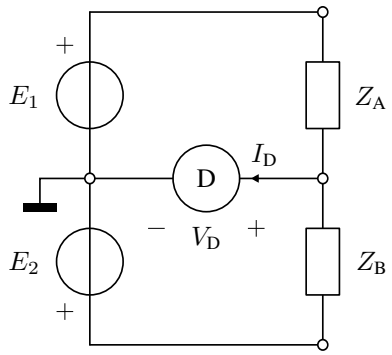

Fig. 1. Schematic diagram of the digital bridge, see text for details.

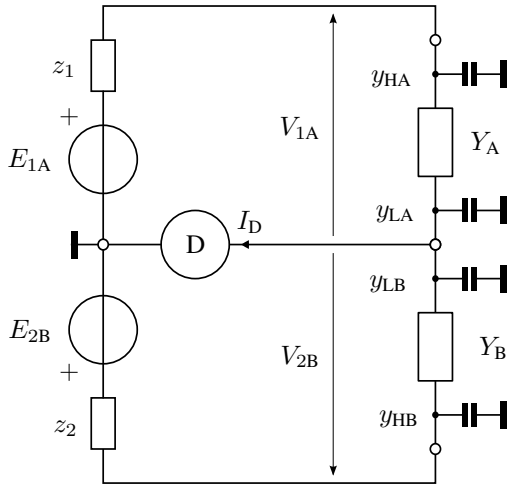

Fig. 2. Circuit model employed in the determination of the measurement model of Sec. II-B (see text for details); thick segments (**—**) represent connections to the shield.

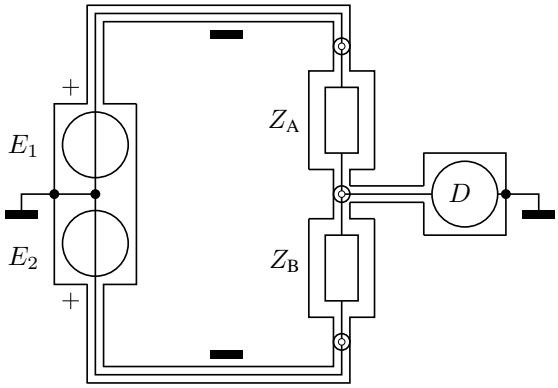

Fig. 3. Coaxial schematic diagram of the digital bridge (see text for details). The black rectangles identify coaxial equalizers.

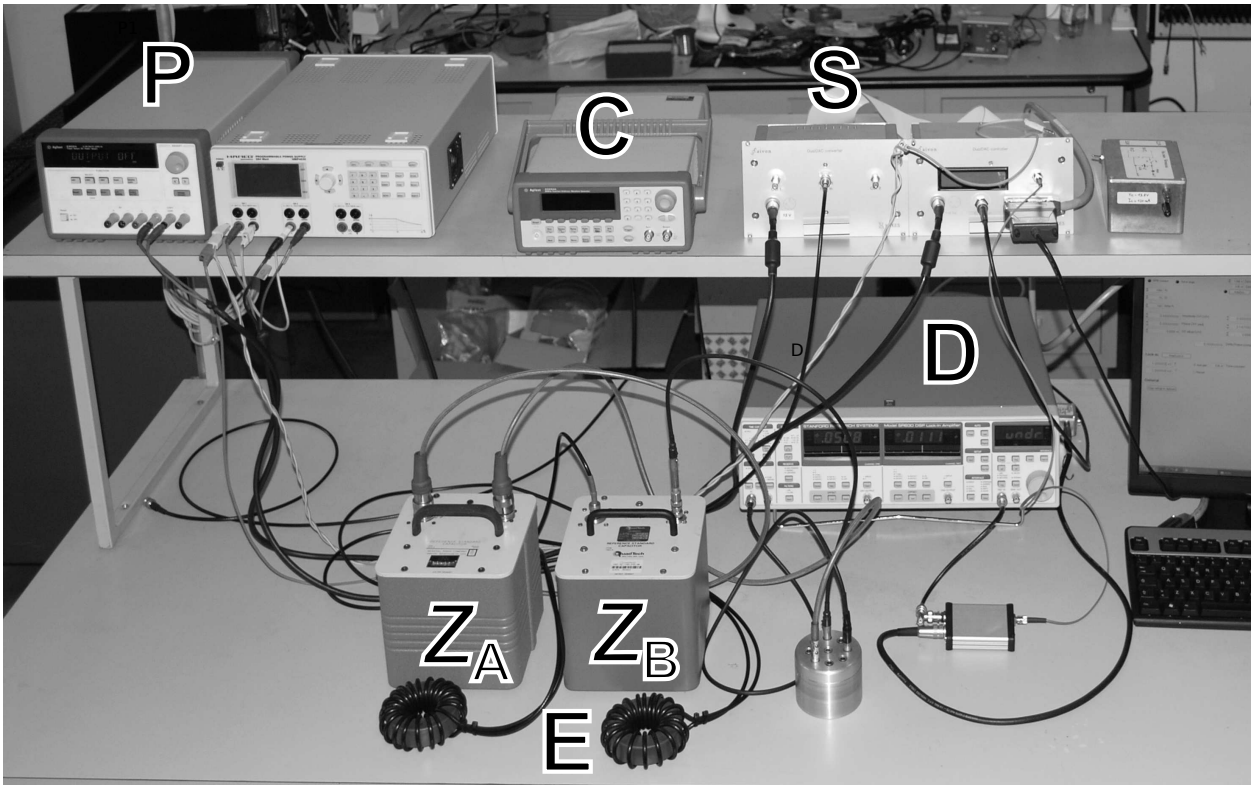

Fig. 4. Picture of the digital bridge showing the impedances Z_A and Z_B under comparison, the source S (energized by power supplies P, one for the analog and one for the digital part), the detector D and the coaxial equalizers E. A 10 MHz clock source C is also shown.

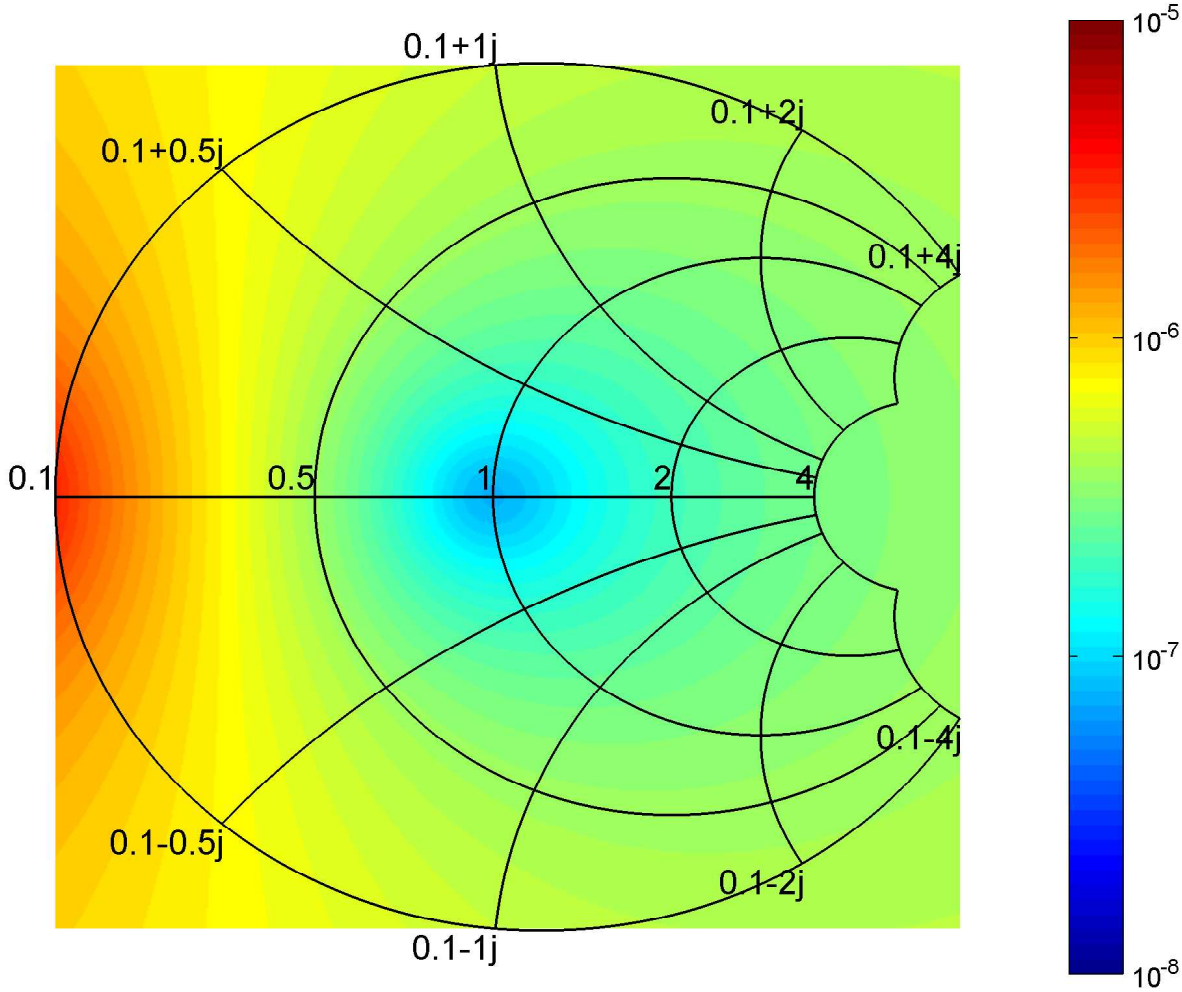

Fig. 5. Color plot of the magnitude of the relative uncertainty of W for $Z_{\mathrm{B}} = 100\,\mathrm{k}\Omega$, and z_k and y_{HX} as given in Tab. III. The plot is given as Smith chart: W coordinates are drawn as black lines; real values of W are along the horizontal diameter; the plot center corresponds to $W = 1 + \mathrm{j}0$ for which the best uncertainty is achieved.

LIST OF TABLES

TABLE I
STANDARDS EMPLOYED DURING THE MEASUREMENTS. THE ASTERISK * DENOTES THE SECOND OF TWO STANDARDS OF THE SAME MODEL.

Label	Description
1 nF, *1 nF	General Radio mod. 1404-A, sealed N_2
10 nF, *10 nF	Custom realization, C0G solid dielectric [16]
100 kΩ	Agilent 42039A
10 kΩ	Agilent 42038A

TABLE II
RESULTS OF COMPARISONS PERFORMED WITH THE BRIDGE.

Z_{A}	Z_{B}	f/Hz	$\mathrm{Re}\,W$	$\mathrm{Im}\,W$	$\mathrm{Re}\,\delta$ $\times 10^6$	$\mathrm{Im}\,\delta$ $\times 10^6$
1 nF	*1 nF	159.24	1.000 324 0	1.83×10^{-6}	0.3	0.1
1 nF	*1 nF	1592.36	1.000 322 6	1.36×10^{-6}	−0.5	−0.1
1 nF	*1 nF	15 873.02	1.000 312 0	2.01×10^{-5}	−15.4	17
10 nF	*10 nF	159.24	0.999 920 0	5.23×10^{-7}	−2.0	0.0
10 nF	*10 nF	1592.36	0.999 922 6	-3.18×10^{-7}	−1.4	0.6
100 kΩ	*10 nF	159.24	1.14×10^{-4}	1.000 568 5	24	5.6
100 kΩ	*1 nF	1592.36	2.60×10^{-4}	1.000 348 6	11	2.1
10 kΩ	*10 nF	1592.36	1.34×10^{-4}	1.000 716 0	24	3.5
10 kΩ	*1 nF	15 873.02	3.71×10^{-4}	0.997 455 9	105	27

TABLE III
UNCERTAINTY BUDGET FOR $W \approx 0 + \mathrm{j}1$, $Z_\mathrm{A} = 100\,\mathrm{k}\Omega$, $Z_\mathrm{B} = 1\,\mathrm{nF}$ AND $f = 1592.36\,\mathrm{Hz}$.

Quantity	X	$u(\mathrm{Re}\,X)$	$u(\mathrm{Im}\,X)$	type
Δg_FR	$0 + \mathrm{j}0$	10^{-6}	10^{-6}	B
z_1, z_2	$(100 + \mathrm{j}40)\,\mathrm{m}\Omega$	$50\,\mathrm{m}\Omega$	$10\,\mathrm{m}\Omega$	B
$y_\mathrm{HA}, y_\mathrm{HB}$	$(0 + \mathrm{j}2)\,\mu\mathrm{S}$	0	$0.5\,\mu\mathrm{S}$	B
$W^{(\mathrm{r})}$	$2.610 \times 10^{-4} + \mathrm{j}1.000\,350\,0$	10^{-7}	10^{-7}	A
W	$2.604 \times 10^{-4} + \mathrm{j}1.000\,348\,6$	6.3×10^{-7}	6.3×10^{-7}	
W^ref	$2.496 \times 10^{-4} + \mathrm{j}1.000\,346\,5$	5.0×10^{-6}	5.8×10^{-6}	
$\delta = W - W^\mathrm{ref}$	$10.8 \times 10^{-6} + \mathrm{j}2.1 \times 10^{-6}$	5.0×10^{-6}	5.8×10^{-6}	